

# Supporting information

## Portable microfluidic biosensing system for real-time analysis of microdialysate in transplant kidneys

Isabelle C. Samper,<sup>‡a</sup> Sally A. N. Gowers,<sup>‡a</sup> Marsilea A. Booth,<sup>a</sup> Chu Wang,<sup>a</sup> Thomas Watts,<sup>a</sup> Tonghathai Phairatana,<sup>a,c</sup> Natalie Vallant,<sup>b</sup> Bynvant Sandhu,<sup>b</sup> Vassilios Papalois<sup>b</sup> and Martyn G. Boutelle<sup>\*a</sup>

<sup>a</sup>Department of Bioengineering, Imperial College London, London, SW7 2AZ, UK

<sup>b</sup>Department of Surgery and Cancer, Imperial College London, London, SW7 2AZ, UK

<sup>c</sup>Institute of Biomedical Engineering, Faculty of Medicine, Prince of Songkla University, Hat Yai, 90110, Thailand

<sup>‡</sup>contributed equally to this work.

### Table of Contents

<b>Figure S1: Wireless potentiostat schematic. ....</b>	<b>S-2</b>
<b>Figure S2: Wireless calibration-controller schematic. ....</b>	<b>S-3</b>
<b>Figure S3: Stability of biosensor response in transit. ....</b>	<b>S-3</b>
<b>Figure S4: Variability of current response between different biosensors. ....</b>	<b>S-4</b>
<b>Figure S5: Variable effect of temperature change on biosensor sensitivity. ....</b>	<b>S-4</b>
<b>Figure S6 Effect of the temperature at the microdialysis probe on the temperature at the biosensors. ....</b>	<b>S-5</b>

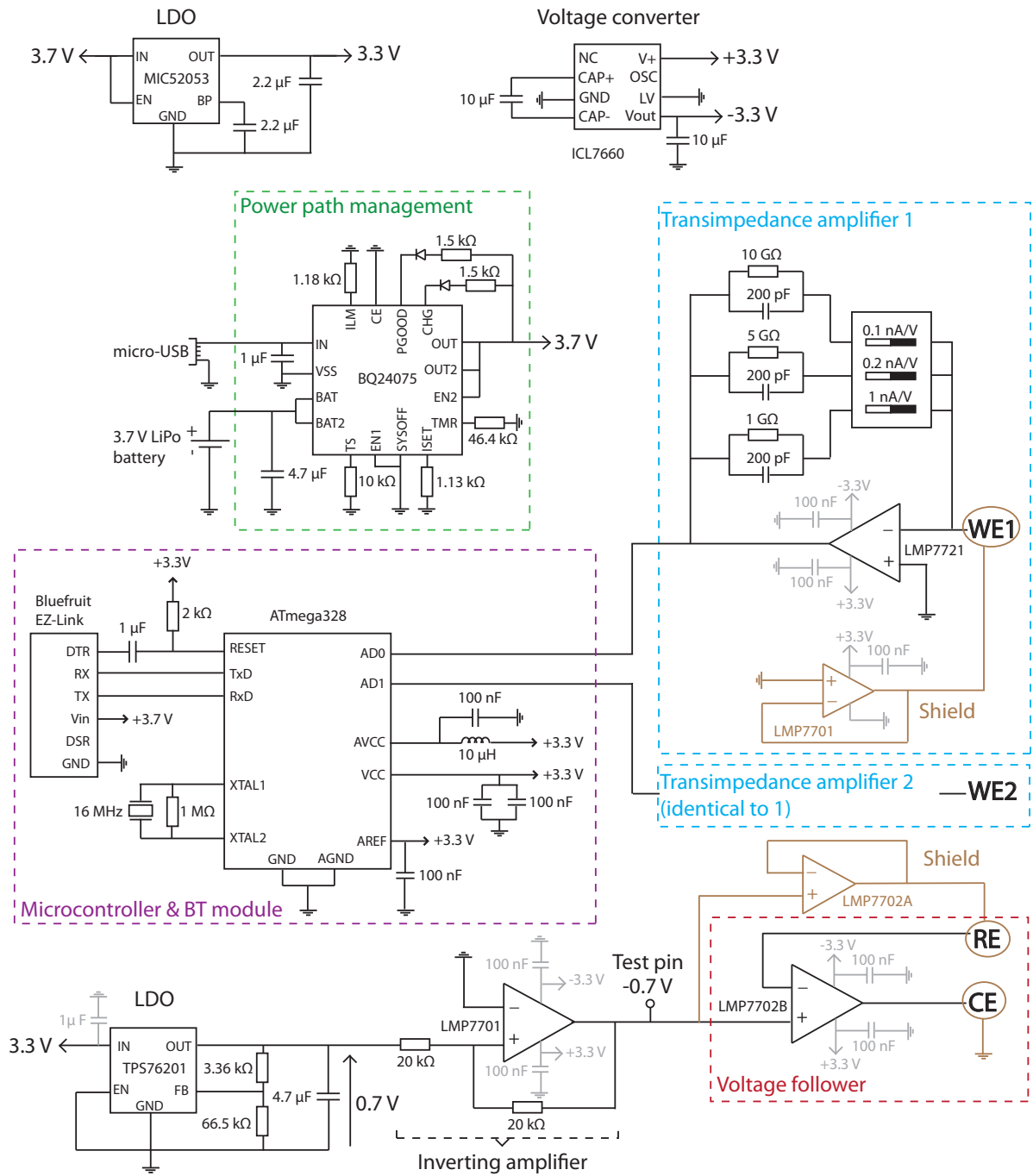


**Figure S1: Wireless potentiostat schematic.** WE1, WE2, RE and CE represent to pins to be connected to working electrodes 1 and 2, the reference and the counter electrodes, respectively. LDO and BT stand for low-dropout regulator and Bluetooth, respectively.

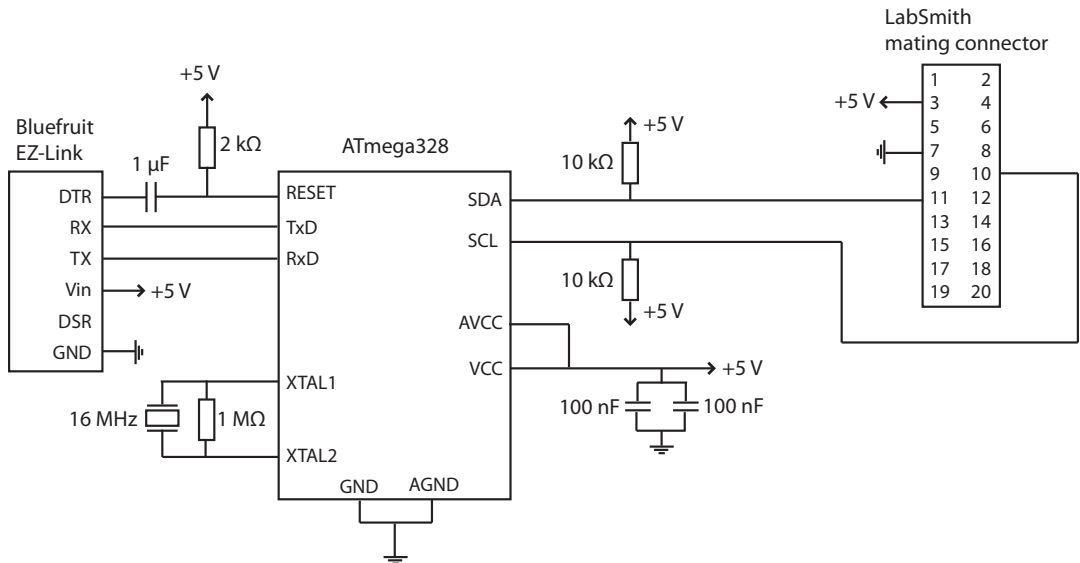


**Figure S2: Wireless calibration-controller schematic.** Schematic of the wireless controller PCB that connects to the LabSmith calibration board. The two main components are the microcontroller (ATmega328) and the Bluetooth module (Bluefruit EZ-Link). The PCB interfaces with the LabSmith breadboard through a 20-pin header (LabSmith mating connector).

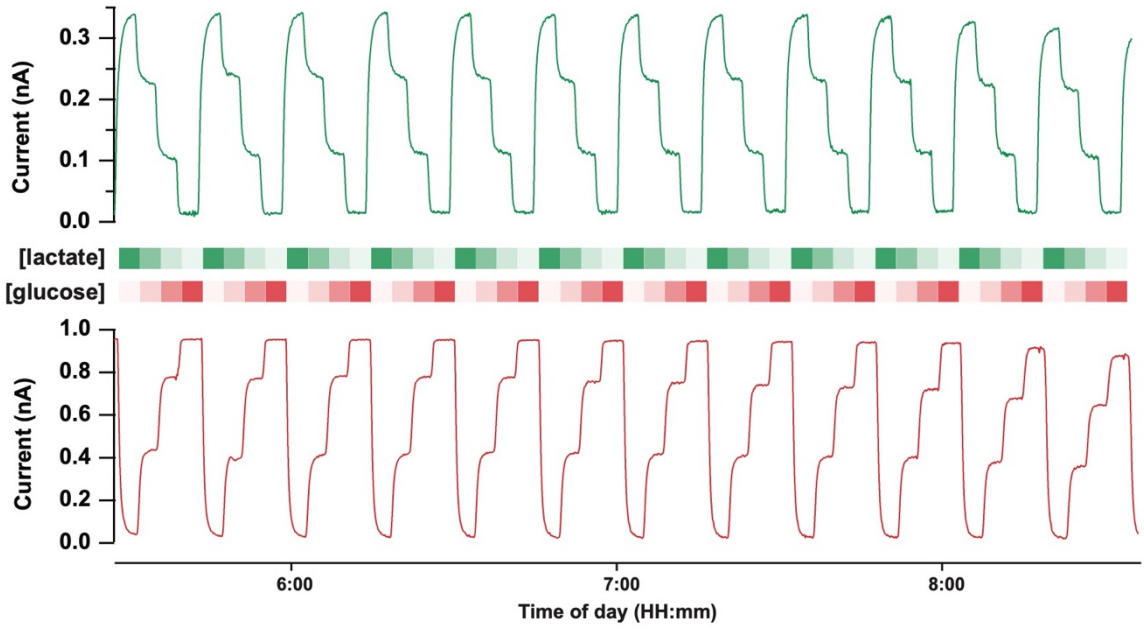


**Figure S3: Stability of biosensor response in transit.** Glucose (red) and lactate (green) biosensor calibration traces recorded in transit over 3 hours while the analysis system was transported from home (because recording started at 5:30 am) to the abattoir. Means of transport employed here include: walking, train, underground and taxi. The four following concentration steps were generated repeatedly at 2  $\mu\text{l}/\text{min}$  using the portable calibration system: 0, 1.67, 3.33 and 5 mM for glucose and 5, 3.33, 1.67 and 0 mM for lactate. Data is shown for 12 consecutive calibration cycles, demonstrating the great reproducibility of calibration in transit for a given biosensor. The currents were recorded online with a 10 Hz sampling rate and smoothed with a Savitzky-Golay 101-point filter.

In the first couple of calibration cycles, the noise in the underlying glucose signal is slightly attenuated at the higher level due to slight clipping of the digital-to-analog converter.

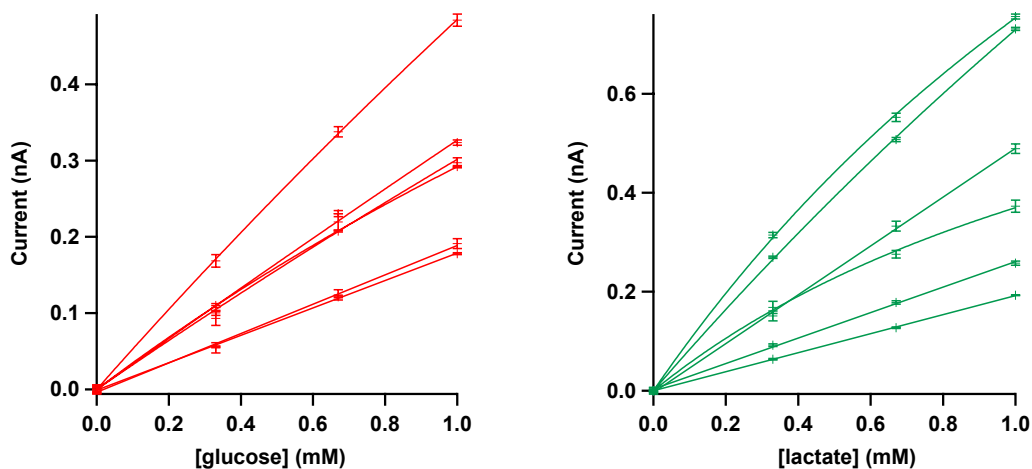


**Figure S4: Variability of current response between different biosensors.** Calibration curves for six glucose (red) and six lactate (green) biosensors recorded in transit using the wireless analysis system. The four concentration steps (0, 0.33, 0.67 and 1 mM) were generated at 2  $\mu\text{l}/\text{min}$  using the portable calibration system. Markers and error bars represent mean and sd of 1-minute measurements. The data was fitted either with a straight line or with Michaelis-Menten equation. The variability between biosensors is due to the inherent variability in the thickness of the polyurethane layer, which is manually dip-coated onto the biosensors.

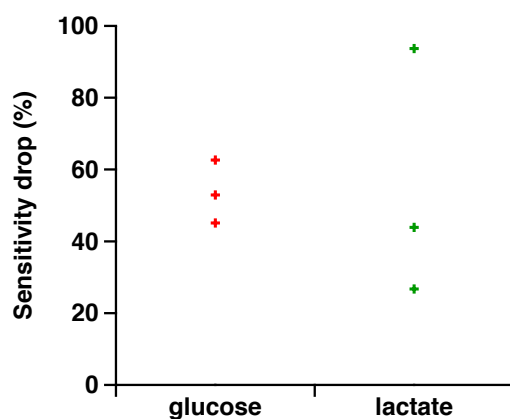


**Figure S5: Variable effect of temperature change on biosensor sensitivity.** Drop in sensitivity measured across 3 glucose and 3 lactate sensors, caused by the temperature changing from 25°C (room temperature) to 1°C (in ice box). The sensitivity of the biosensors is calculated from calibrations run in a constant 2  $\mu\text{l}/\text{min}$  flow (6 steps, 0-1 mM) using the automated calibration board. The decrease in sensitivity is expressed in percentage of the sensitivity measured at 25°C.

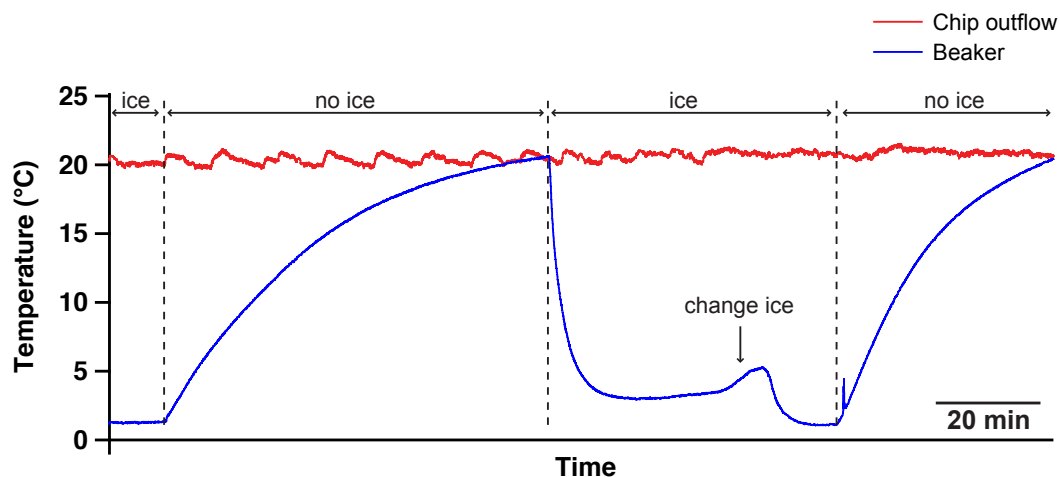


**Figure S6 Effect of the temperature at the microdialysis probe on the temperature at the biosensors.** The blue trace shows the temperature measured in a beaker where the microdialysis probe was inserted. The red trace shows the temperature measured in the downstream microfluidic chip outflow where the biosensors were placed. The microfluidic chip was connected to the outlet of the microdialysis probe using a 50 cm tubing extension, reproducing the kidney monitoring setup. The beaker temperature was varied by placing it in and out of ice water, indicated at the top of the graph. The vertical arrow points out a time where the ice surrounding the beaker was changed for fresh ice as it had started to melt. The temperature in the microfluidic chip remains constant throughout despite the change at the microdialysis probe.